Fuel 165 (2016) 235–243

Contents lists available at ScienceDirect

Fuel

journal homepage: www.elsevier.com/locate/fuel

Evaluation of CaO-decorated Fe_2O_3/Al_2O_3 as an oxygen carrier for in-situ gasification chemical looping combustion of plastic wastes

Jinxing Wang, Haibo Zhao *

State Key Laboratory of Coal Combustion, Huazhong University of Science and Technology, Wuhan 430074, Hubei, People's Republic of China

HIGHLIGHTS

- iG-CLC of plastic waste was proposed to control the formation of PCDD/Fs.
- 5 wt.% CaO-decorated Fe_2O_3/Al_2O_3 was used for dechlorination.
- Optimizing operation conditions mitigate undesirable influence of CaO decoration.
- Cl element accumulation and little ash deposition on OC surface were observed.

ARTICLE INFO

Article history:
Received 7 May 2015
Received in revised form 7 August 2015
Accepted 8 October 2015
Available online 24 October 2015

Keywords:
In-situ gasification chemical looping combustion
Plastic waste
CaO-decorated Fe_2O_3/Al_2O_3
PCDD/Fs
Chemical looping dechlorination

ABSTRACT

The use of solid waste such as plastic waste in Chemical Looping Combustion (CLC) becomes interesting, with potential advantages of exploiting new energy sources, suppressing pollutants, and capturing carbon dioxide. However, the emission of polychlorinated dibenzo-p-dioxins and dibenzofurans (PCDD/Fs) which as toxic matter has aroused increasing attention during the utilization process of these solid wastes, especially for plastic waste which contains a high chlorine content. Through applying CaO decoration to Fe-based oxygen carrier (OC) is it possible to realize effective dechlorination during chemical looping processes. In this study, a 5 wt.% CaO-decorated Fe_2O_3/Al_2O_3 as OC was used for in-situ gasification chemical looping combustion (iG-CLC) of plastic waste, and the reactivity of the decorated OC particles was tested in a batch fluidized-bed reactor, compared with that of raw Fe_2O_3/Al_2O_3 OCs. Operation conditions, including reaction atmosphere, supply oxygen ratio and reaction temperature, were investigated to explore their influence on carbon conversion, maximum instantaneous rate of fuel conversion and CO_2 yield. Results indicated that CaO decoration results in a lower reactivity of OC particles. However, by optimizing these operation conditions the undesirable influence of CaO decoration can be mitigated. The stability of OC reactivity was evaluated through 10 redox cycles, where stable carbon conversion, maximum instantaneous rate of fuel conversion and CO_2 yield were observed. These used OC particles were characterized by a surface area and porosity analyzer and an Environment Scanning Electron Microscope coupling with Energy Dispersive X-ray spectroscopy (ESEM–EDX). The specific surface area (BET) result indicated that CaO-decorated OC particles present lower BET and pore volume after 10 redox cycles, and the ESEM–EDX result also demonstrated little ash deposition on the surface of OC particles, which both contribute to the slight deterioration of OC reactivity. It was also observed from ESEM–EDX that there is the accumulation of Cl element on OC surface, providing sound evidence for dechlorination during the iG-CLC of plastic waste.

1. Introduction

Chemical Looping Combustion (CLC) has been regarded as a very promising technology for inherent separation of greenhouse gas CO_2 during fuel combustion. So far, extensive researches have focused on the utilization of solid fuels in CLC, which have been widely proven to be feasible in different prototype reactors [1–4]. Currently there are three main strategies for CLC with solid fuels [5]. The first is using synthetic gas from the gasification of solid fuels in the fuel reactor [5,6]. The second is direct introduction of solid fuels to the fuel reactor where the gasification of solid fuel and subsequent reduction reactions with the oxygen carrier (OC)

* Corresponding author. Tel.: +86 27 8754 4779x8208; fax: +86 27 8754 5526.
E-mail addresses: wangruoguang860928@126.com (J. Wang), klinsmannzhb@163.com, hzhao@mail.hust.edu.cn (H. Zhao).

http://dx.doi.org/10.1016/j.fuel.2015.10.020
0016-2361/

particles will occur simultaneously, namely in-situ gasification chemical looping combustion (iG-CLC) [7,8]. The third is to use an OC which releases O_2 in the fuel reactor and actually burns the fuel with gas-phase oxygen. The last alternative is referred to as chemical-looping with oxygen uncoupling (CLOU) [9,10].

To find suitable oxygen carriers (OCs) is a key issue for the development of the CLC technology [11]. There have been a number of publications on evaluation of the OC particles, e.g., the oxides of Fe, Ni, Mn, Co and Cu [12–15]. In order to increase the reactivity and durability of the particles, they are often supported with some inert materials like Al_2O_3 [1]. Thermodynamically, the Cu-based, Co-based and Mn-based OCs are the most favorable OCs for the CLOU process [15]. Among these OC materials for CLOU, Cu-based OCs were investigated extensively because of their greater oxygen transport capacity, high reactivity and low cost [15]. However, the use of Cu-based OCs is also challenging due to its low melting point [16]. Of the listed OC materials, Ni-based OC results in a small presence of CO and H_2 in the flue gas of the fuel reactor because CO and H_2 cannot be completely oxidized by NiO in thermodynamics [17]. Fe-based OC is selected in this study for low cost, environmental friendliness, low agglomeration or attrition rate and stable reactivity compared to other metal oxides [18], and, more importantly, thermodynamic impracticability in reactivity with HCl.

During recent years, solid waste has become an interesting fuel because it has significant environmental benefits [19]. Plastic waste as a major category of solid waste is considered potentially applicable as fuel due to its high heating values [20]. However, the utilization of plastic waste is not always environmentally feasible because of potential secondary pollution, such as the emission of polychlorinated dibenzo-p-dioxins and dibenzofurans (PCDD/Fs). Numerous researchers are in complete agreement that the formation mechanisms of PCDD/Fs include two major routes [21,22]: (1) PCDD/Fs formation by heterogeneous catalysis condensation reaction of direct precursors like chlorobenzene and chlorophenol; (2) PCDD/Fs formation through an oxidative breakdown of macromolecular carbon structures, namely de novo synthesis from simple hydrocarbon and chlorine. On the one side, CLC, which utilizes active lattice oxygen provided by an OC for fuel oxidation in the absence of O_2, provides a promising route to suppress the de novo route of PCDD/Fs formation [23]. On the other side, a high chlorine content in plastic waste may contribute to the formation of PCDD/Fs in the furnace effluent [20], either directly or indirectly. Consequently, it is essential to explore effective ways for dechlorination during the utilization process of plastic waste based on the formation mechanisms of PCDD/Fs. To our knowledge, little attention has been paid to the application of some adsorbents for dechlorination in the CLC process of plastic waste, although the feasibility of dechlorination have been illustrated through alkaline adsorbents ($CaCO_3$, CaO, $Ca(OH)_2$) for conventional combustion in the previous achievements [20,24,25].

This work focuses on iG-CLC of plastic waste using Fe-based OCs. The schematic of an iG-CLC configuration is shown in Fig.1. In the fuel reactor (FR), a mixture of OC and plastic waste is fluidized by a gasification agent which usually contains steam [18,26]. According to reactions (1)–(3), initially plastic waste quickly releases volatiles, then char is gasified by steam at high temperatures. CO, H_2 and CH_4 are the main gasification products generated in this process. The gasification products and volatiles are then oxidized by the OC. Reactions (4)–(6) show the OC reduction reaction with the main products of plastic waste devolatilisation and gasification. Subsequently, the OC is transferred to the air reactor (AR), where it is reoxidized (see (R7)) and sent back to the FR to start a new redox cycle. If some adsorbents can be integrated with OC particles to realize the dechlorination and these adsorbent-decorated OC particles can still present a reliable reactivity during the iG-CLC process of plastic waste, costly equipment and energy consumption for dechlorination can be avoided on this premise of the harmless utilization of plastic waste. It is worth noting that, although the dechloridation and combustion efficiencies have been comprehensively investigated for the CLC of HCl-containing synthesis gas in our recent publication [23], it is still essential to study the reliable reactivity during the iG-CLC process of plastic waste due to the intrinsic difference between synthesis gas and plastic waste.

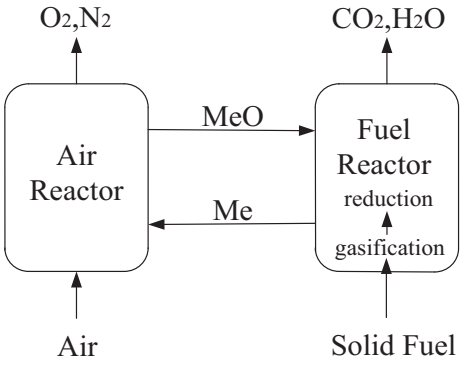

Fig. 1. The schematic of CLC process.

Plastic waste pyrolysis $\rightarrow$ volatiles + Char (R1)

$C + H_2O = CO + H_2$ (R2)

$CO + H_2O = CO_2 + H_2$ (R3)

$CO + 3Fe_2O_3 = CO_2 + 2Fe_3O_4$ (R4)

$H_2 + 3Fe_2O_3 = H_2O + 2Fe_3O_4$ (R5)

$CH_4 + 12Fe_2O_3 = CO_2 + H_2O + 8Fe_3O_4$ (R6)

$4Fe_3O_4 + O_2 = 6Fe_2O_3$ (R7)

One purpose of this study was to evaluate the reactivity of CaO-decorated Fe-based OC particles in a batch fluidized bed reactor in terms of carbon conversion, maximum instantaneous rate and CO_2 yield. The second purpose was to examine the feasibility of dechlorination during the iG-CLC process of plastic waste using an Environmental Scanning Electron Microscope coupled with an Energy Dispersive X-ray spectroscopy system (ESEM–EDX, FEI Quanta 2000). In these experiments, the Fe-based OCs, 60 wt.% Fe_2O_3/40 wt.% Al_2O_3, were synthesized by the co-precipitation method and subsequently 5 wt.% CaO (mass ratio of CaO to OCs) was used to decorate these OC particles through wet impregnation. Note that using 40 wt.% Al_2O_3 as support has been demonstrated to give stable conversion and good reactivity [27,28]. In our recent publication [23], wet impregnation has been considered as the optimizing decoration method and 5 wt.% CaO loading reached an optimized level of dechloridation. The CLC performance of the CaO-decorated Fe_2O_3/Al_2O_3 OC particles was compared with that of the raw Fe_2O_3/Al_2O_3 OC particles to examine the effect of CaO decoration. It is expected that this study can provide useful information on the chemical looping utilization of plastic waste.

2. Experimental section

2.1. Materials

A medical perfusion tube as a typical plastic waste was selected for this study. First, the sample was dried in an oven at 105 °C for 24 h. Next, it was milled and sieved to 0.5–0.6 mm prior to tests. Table 1 summarizes the proximate and ultimate analysis and lower

Table 1
Proximate analysis, ultimate analysis (on wt.%, as received) and lower heating value of the medical plastics.

Sample	Proximate (wt.%, as received)				LHV (MJ/kg, db)	Ultimate (wt.%, d.a.f)					
	M	FC	V	A		C	H	N	S	O	Cl
Medical plastics	0.03	0.08	93.79	6.1	33.87	73.89	10.82	0.72	0.16	3.39	4.92

Table 2
Ash analysis of the medical plastics (on wt.%, as received).

Sample	Component analysis (wt.%)								Else elements
	Al_2O_3	SiO_2	SO_3	CaO	Mn_2O_3	Fe_2O_3	CuO	ZnO	
Medical plastics	15.63	34.92	4.48	19.54	1.39	19.23	1.89	2.39	0.53

heating value of medical plastic, and its ash analysis is listed in Table 2.

The OC was synthesized by co-precipitation route using Fe$(NO_3)_3{\cdot}9H_2O$ (ACS reagent, purity >98.5 wt.%) and Al$(NO_3)_3{\cdot}9H_2O$ (ACS reagent, purity >98.5 wt.%) as original materials. The prepared mixture solution of Fe/Al metal nitrates ensured that Fe_2O_3/Al_2O_3 mass ratio was fixed at 60 wt.%: 40 wt.%. In the process, the aqueous solution of ammonia was slowly added into the obtained solution until the pH value reached to 9–10. The mixture was stirred at 90 °C in the thermostatic stirring apparatus for 3 h and the metal complex was precipitated. The obtained precipitate was dried in air at 105 °C for 24 h and then calcined in a muffle furnace at 1000 °C for 6 h. These nitrates turned into corresponding metal oxide, and finally the generated OC particles were sieved to the size range of 0.2–0.3 mm.

$Ca(NO_3)_2{\cdot}4H_2O$ (purity >99.0 wt.%; size <5 μm) was selected as adsorbent precursor, and the wet impregnation method was adopted for decorating these OC particles. First, the adsorbent precursor was dissolved in 100 mL deionized water, and then the prepared raw Fe-based OC particles were soaked in this solution. Next, the mixture was stirred for 12 h at ambient temperature and dried in the air at 105 °C. Last, $Ca(NO_3)_2{\cdot}4H_2O$ turned into CaO after it was calcined in air at 1100 °C for 3 h, and they were received to the uniform particles from 0.2 mm to 0.3 mm. During the wet impregnation process, a mass ratio of CaO to OCs (CaO/OC), 5 wt.%, was designated.

2.2. Apparatus and procedure

The experimental tests for the iG-CLC of plastic waste were conducted in a laboratory-scale fluidized bed. A detailed description of this system can be found elsewhere [25,29–31]. In these experiments, a mixed gas of steam and N_2 was used as the fluidizing agent, and the flow of fluidizing agent was 600 mL/min. Deionized water was introduced into the steam generator with a constant flow pump (TBP5002, Shanghai Tauto Biotech), preheating the water to 350 °C. The steam flow rate was controlled by the flow rate of water through the pump. Initially, 30 g of OC particles were fed into the reactor through the hopper located on the top of the tube and fluidized by pure air at an established temperature for 30 min to ensure thorough oxidation. Determinated mass of plastic waste were inserted into the hopper in stable conditions and then pushed into the reactor by pressurized nitrogen gas. The off gas from the top of reactor was first led to a filter to remove particulate matter and an electric cooler to remove the steam carried by gas, and then to on-line gas analyzer (Gasboard-3151) to detect the concentration of CO_2, CO, CH_4, H_2 and O_2. Concentration values were instantaneously recorded by a data logger connected to the computer. After these experiments, the crystalline phase was detected by a X-ray diffraction (Shimadzu, XRD-7000), the surface area of the OC was determined using the BET method by adsorption/desorption of nitrogen at 77 K in a Surface Area and Porosity Analyzer (Micromeritics ASAP3000) and the morphologies and surface composition of OC particles were examined using an Environmental Scanning Electron Microscope coupled with an Energy Dispersive X-ray spectroscopy system (ESEM–EDX, FEI Quanta 2000).

To investigate the effect of the mass of plastic waste fed on the reactivity of OCs in CLC, the supply oxygen ratio, ϕ, was introduced in this work and it can be calculated by

$$\phi = \frac{n_{O,OC}}{n_{O,plastic.waste}} \tag{1}$$

where $n_{O,OC}$ is the molar amount of oxygen in the OCs available for the CLC process and $n_{O,plastic.waste}$ is the molar amount of oxygen needed for full combustion of plastic waste.

$$n_{O,OC} = m_{OC} \times \frac{\beta_{Fe_2O_3}}{3M_{Fe_2O_3}} \tag{2}$$

$$n_{O,plastic.waste} = m_{plastic.waste}\left(\frac{0\beta_N}{M_N} + \frac{2\beta_C}{M_C} + \frac{2\beta_S}{M_S} + \frac{\beta_H}{2M_H} - \frac{\beta_O}{M_O} - \frac{\beta_{Cl}}{2M_{Cl}}\right) \tag{3}$$

here β_i is the mass fraction of active component i(Fe_2O_3) in the OCs or (N, C, S, H, O, Cl) in the plastic waste, m_{OC} is the mass of the oxidized the OC, $m_{plastic.waste}$ is the mass of the plastic waste fed into the reactor, and M_i is the molar mass of species i. Eq. (3) was based on the assumption that plastic waste is only oxidized to N_2, CO_2, SO_2 and H_2O in the FR by OCs and HCl is the only form of chlorine-containing reactants.

2.3. Data evaluation

Carbon conversion in the system relies mainly on the combined process of plastic waste pyrolysis and OC reduction with plastic waste syngas in the FR rather than on the process of residual char combustion in the AR, especially for the high-volatile plastic waste. It is noted that the effect of residual char combustion in the AR can be ignored because plastic waste contains a lower FC_{ad} content (shown in Table 1). In the FR the molar flow of inlet N_2 (F_{N_2}) under the standard conditions is known, and the molar flow of gaseous product species i, $F_{i,out}$ (i = CO_2, CO, CH_4, H_2) can be calculated by N_2 mass balance as follows:

$$F_{i,out}(t) = \frac{F_{N_2}}{(1 - \sum_i y_i)} y_i \tag{4}$$

where y_i is the molar fraction of component i(CO, CO_2, CH_4, H_2) in the outlet gas flow on a dry basis.

The carbon conversion, $X_C(t)$, is calculated by integrating the ratios of mole of carbon in the flue gas to the mole of carbon added to the reactor ($N_{C,fuel}$).

$$X_C = \frac{\int_0^t (F_{CO,out} + F_{CO_2,out} + F_{CH_4,out})dt}{N_{C,fuel}} \times 100\% \quad (5)$$

where t is the duration of monitoring outlet gases (y_i, $i = CO_2$, CO, CH_4, H_2). And $N_{C,fuel}$ is the mole of carbon fed to the reactor.

The instantaneous rate of fuel conversion, $r_{C,inst}$, is calculated as the gasification rate per unit of non-gasified carbon in the reactor. In this study, the maximum instantaneous rate, $r_{C,inst,max}$, is selected for evaluating the reaction process.

$$r_{C,inst}(t) = \frac{1}{1 - X_C} \frac{dX_C}{dt} \times 100\% \quad (6)$$

The CO_2 yield, η_{CO_2} , is calculated as the ratio of CO_2 concentration to the total carbon concentration in the FR flue gas.

$$\eta_{CO_2} = \frac{\int_0^t F_{CO_2,out} dt}{\int_0^t (F_{CO,out} + F_{CO_2,out} + F_{CH_4,out})dt} \quad (7)$$

3. Result and discussion

3.1. Comparison with raw Fe_2O_3/Al_2O_3

To determine the effect of CaO decoration on the reactivity of OC particles, the same experiments were conducted in a batch fluidized bed reactor using raw Fe_2O_3/Al_2O_3 or CaO-decorated Fe_2O_3/Al_2O_3 as OCs at a reactor temperature of 900 °C. The supply oxygen ratio was 1, and the fluidization gas contained 40% steam and 60% N_2. The volume concentrations of the main gaseous components in iG-CLC of plastic waste were respectively shown in Fig. 2(a) and (b). The peaks of CO_2, CO and H_2 were presented in the initial 100s for both OCs. Notably, no CH_4 was measured continuously in the present setup. In chemical looping systems, CH_4 undergoes indirect combustion and most likely starts with its partial oxidation to produce H_2 and CO [32]. Another reasonable explanation is the decomposition of CH_4 under high temperature [33]. Among them CO_2 should be mainly derived from the release of volatiles and the reaction of syngas with the Fe_2O_3/Al_2O_3 OC particles. When using raw Fe_2O_3/Al_2O_3 OCs, little CO and H_2 still exist in the exhaust gas, which indicated that the OC particles cannot fully oxidize these combustible gases due to limited residence time in the batch fluidized bed reactor. In general, CO and H_2 are mainly originated from the pyrolysis of plastic waste and the release of volatiles [34], and the segregation of volatile matter from plastic particles is expected to cause the poor contact between OC particles and volatile matter. Another factor is that the suspension of some plastic particles (with relatively low density) in the FR leads to by-pass of some gasification/pyrolysis products and short residence time [35]. Note that higher CO and H_2 peak values were shown in Fig. 2(b) when using 5 wt.% CaO-decorated OCs. A reasonable explanation is that partial active oxides were hindered by CaO adsorbent, restraining the transfer of active lattice oxygen and then the oxidation of partial combustible gases. It is expected that the negative effect of CaO decoration on the reactivity of OCs can be weakened through optimizing operating conditions, including reaction atmosphere, supply oxygen ratio and reaction temperature.

3.2. Effect of reaction atmosphere

The effect of reaction atmosphere on carbon conversion, maximum instantaneous rate and CO_2 yield for the iG-CLC of plastic waste using 5 wt.% CaO-decorated Fe_2O_3/Al_2O_3 were investigated at 900 °C and supply oxygen ratio was1. For reaction atmosphere, the steam content was varied between 0%, 20%, 40% and 60%. Fig. 3(a) presents that more steam content contributes to a higher carbon conversion, especially when compared with pure N_2 atmosphere. The possible reason is that more steam can promote residual coke gasification [8]. Note that the maximum instantaneous rate obviously decreases with the increase of steam content, as shown in Fig. 3(b). Generally, H_2 and CO can be considered as the main combustible components [36]. More steam can restrain the reaction of R5, resulting in more H_2 existing in reaction atmosphere. The existence of the pyrolysis components would hinder the following devolatilisation [37,38], which could be mainly responsible for this phenomenon. Thermodynamically, the amount of steam during the gasification process was in excess to decrease external mass transfer, and the high steam concentration may also have detrimental effect on the reduction of OCs [35]. Fig. 3(c) showed that more steam content gives rise to higher CO_2 yield with the exception of 60% H_2O. The inhibition of devolatilisation

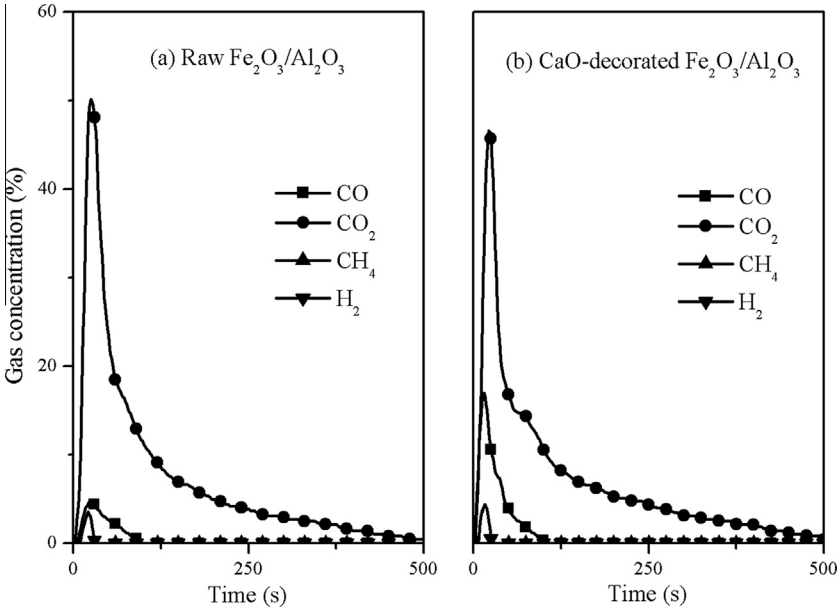

Fig. 2. Volume concentrations of main gaseous components in the iG-CLC of plastic waste using (a) raw Fe_2O_3/Al_2O_3 and (b) CaO-decorated Fe_2O_3/Al_2O_3.

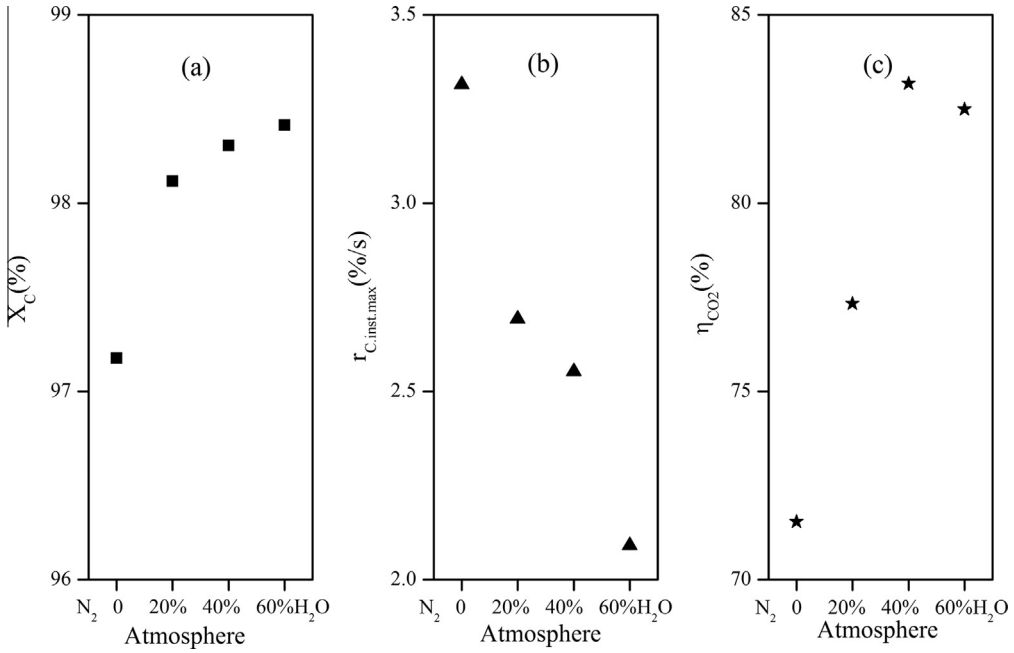

Fig. 3. Carbon conversion (a), maximum instantaneous rate (b) and CO_2 yield (c) for 5 wt.% CaO-decorated Fe_2O_3/Al_2O_3 with different reaction atmospheres.

from steam can extend the residence time for these pyrolysis gases, resulting in more sufficient oxidation of combustible gases. For 60% steam content, the lower CO_2 yield (compared with 40% steam content) should be derived from the inferior reductions of OCs with these pyrolysis gases.

3.3. Effect of supply oxygen ratio

The effect of supply oxygen ratio was also evaluated. And these iG-CLC experiments of plastic waste were conducted at 900 °C, and the fluidization gases contained 40% steam and 60% N_2. Fig. 4 shows carbon conversion, maximum instantaneous rate and CO_2 yield of plastic waste using 5 wt.% CaO-decorated Fe_2O_3/Al_2O_3 with different supply oxygen ratios (1, 1.5, 2, 2.5). As shown in Fig. 4(a), more than 98.3% of carbon conversion can be obtained when the supply oxygen ratio was 1, which indicates that the effect of supply oxygen ratio on carbon conversion was not significant. This should be related to the low FC_{ad} content (seen in Table 1). It can be found that a higher supply oxygen ratio improved the maximum instantaneous rate in Fig. 4(b). One reasonable explanation is that more OC particles can enhance the opportunity of OC particles reacting with combustible gases and subsequently the consumption of the gasification intermediates by OCs eliminates the inhibition effect of gasification products [35], accelerating the devolatilisation. Another minor reason is that a small supply oxygen ratio may lead to the emergence of FeO and Fe, resulting in a lower reactivity of

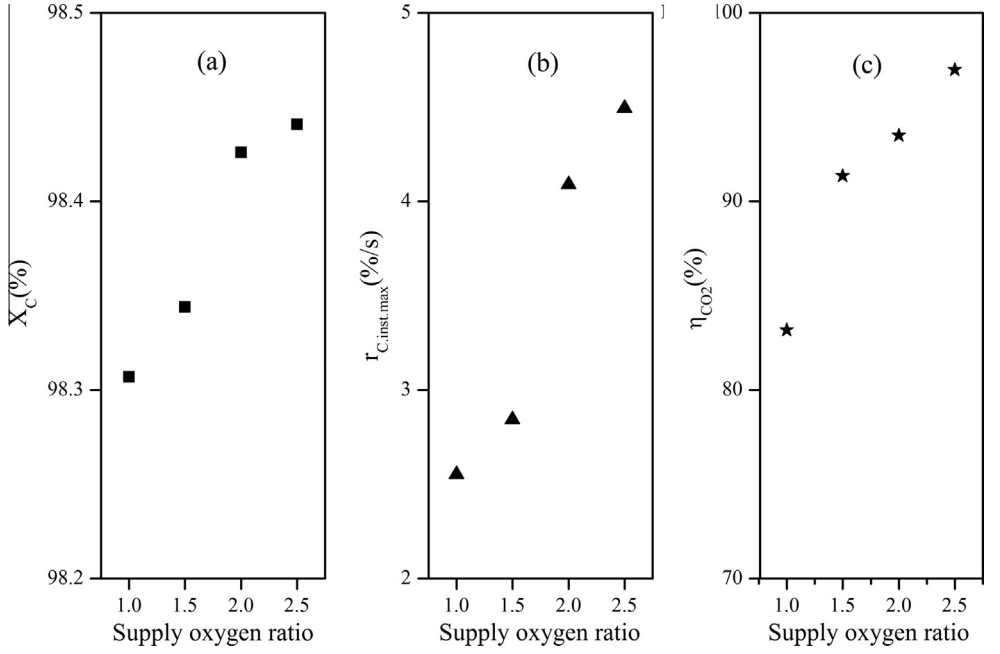

Fig. 4. Carbon conversion (a), maximum instantaneous rate (b) and CO_2 yield (c) for 5 wt.% CaO-decorated Fe_2O_3/Al_2O_3 with different supply oxygen ratios.

OC particles in thermodynamics [35,39]. Fig. 4(c) shows that CO_2 yield can be improved with the increase of supply oxygen ratio. Note that CO_2 yield can reach 97% when the supply oxygen ratio was 2.5, which should be an acceptable value in iG-CLC.

3.4. Effect of reactor temperature

Four reaction temperatures, 850 °C, 875 °C, 900 °C, 925 °C, were chosen to investigate the effect of temperature on carbon conversion, maximum instantaneous rate and CO_2 yield using 5 wt.% CaO-decorated Fe_2O_3/Al_2O_3OC particles. The supply oxygen ratio was 2.5 and the fluidization gases contained 40% steam and 60% N_2. As shown in Fig. 5(a) and (b), carbon conversion and maximum instantaneous rate at high temperatures were generally higher than those at low temperatures. Generally, volatiles are, due to the high temperature, rapidly released when the plastic waste particles were introduced in the reactor and can therefore react directly with the metal oxide. Higher temperature can accelerate the release of volatile [40,41] and subsequent oxidation of combustible gases promotes carbon conversion, especially for plastic waste containing a high volatile content (93.79%). Hence higher temperatures eventually improve CO_2 capture efficiencies with the exception of 925 °C, as shown in Fig. 5(c). Inevitably, more combustible gases exist in exhaust gas due to the faster release of volatile and shorter residence time at higher temperatures, which finally leads to a lower CO_2 yield at 925 °C than at 900 °C.

3.5. Experiments with multiple redox cycles

Ten successive cycles experiments were conducted at 900 °C using two kinds of OC particles to test the durability of these CaO-decorated OC particles reactivity and the raw Fe_2O_3/Al_2O_3 OC particles was used as a reference. The supply oxygen ratio was 2.5 and the fluidization gases contained 40% steam and 60% N_2. As shown in Fig. 6(a) and (b), the average values of carbon conversion and maximum instantaneous rate for CaO-decorated OCs are not far below those of raw Fe_2O_3/Al_2O_3OCs. Note that the CO_2 capture efficiencies (shown in Fig. 6(c)) obtained using CaO-decorated Fe_2O_3/Al_2O_3 OCs are not less than 97%, which can be accepted in the iG-CLC of plastic waste although they are still lower than those of raw Fe_2O_3/Al_2O_3 OCs. Thus, these results indicated that CaO-decorated Fe_2O_3/Al_2O_3 as OC can be used for the iG-CLC of plastic waste.

3.6. Physicochemical characterization

To analyze crystalline phase after single reduction under the optimized condition (reaction atmosphere contained 40% steam and 60% N_2, supply oxygen ratio was 2.5 and temperature was 900 °C), the used raw Fe_2O_3/Al_2O_3 and CaO-decorated Fe_2O_3/Al_2O_3 OC particles were examined by the X-ray diffraction. Also, in order to evaluate the effect of CaO decoration on the surface area and to examine the morphologies and surface composition of OC particles, two kinds of OC particles after ten successive cycles under the optimized condition were respectively detected by a Surface Area and Porosity Analyzer and an Environmental Scanning Electron Microscope coupled with an Energy Dispersive X-ray spectroscopy system.

3.6.1. Crystalline phase analysis

As shown in Fig. 7(a) and (b), there were three main phases: Fe_2O_3, Fe_3O_4 and Al_2O_3 in these two kinds of OC particles except for CaO derived from adsorbent decoration. Compared with raw Fe_2O_3/Al_2O_3 (shown in Fig. 7(a)), it can be seen that no new phases of Fe are produced after reduction reaction for CaO-decorated Fe_2O_3/Al_2O_3 in Fig. 7(b). These XRD results demonstrate the residue of active Fe_2O_3, indicating that the incomplete conversion of CO and H_2 should be derived from the poor contact between OC particles and combustible gases, which is consistent with the statement in Section 3.1.

3.6.2. BET analysis

The BET specific surface area and pore volume of fresh and used Fe_2O_3/Al_2O_3 OCs with or without 5 wt.% CaO decoration after ten successive cycles were tested. First, it was obtained that the BET area and pore volume (BET = 3.49 m^2/g; Pore volume = 21.72 $\times$ 10^{-3} cm^3/g) of fresh Fe_2O_3/Al_2O_3 OCs after CaO decoration is greater than that (BET = 2.75 m^2/g; Pore volume = 19.71 $\times$ 10^{-3} cm^3/g)

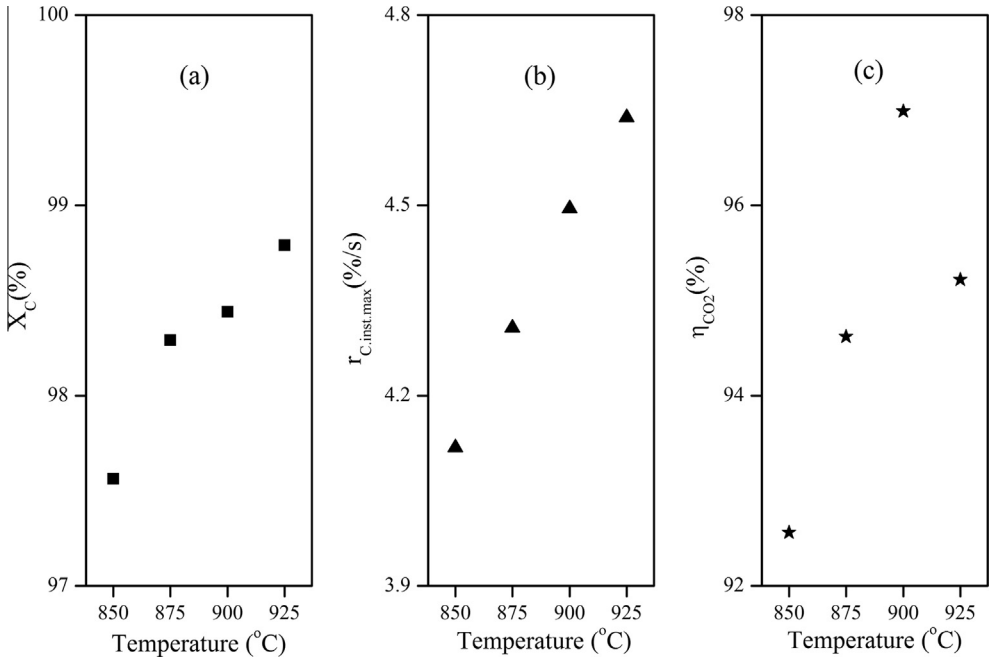

Fig. 5. Carbon conversion (a), maximum instantaneous rate (b) and CO_2 yield (c) for 5 wt.% CaO-decorated Fe_2O_3/Al_2O_3 with different reaction temperatures.

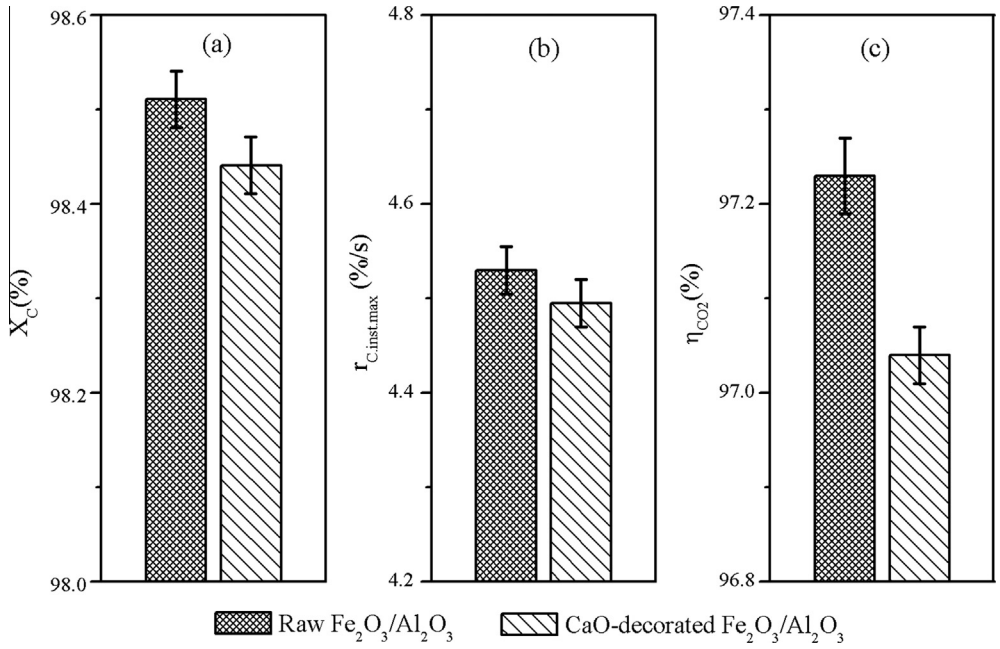

Fig. 6. Carbon conversion (a), maximum instantaneous rate (b) and CO_2 yield (c) in the iG-CLC of plastic waste using raw Fe_2O_3/Al_2O_3 and CaO-decorated Fe_2O_3/Al_2O_3 within ten successive cycles.

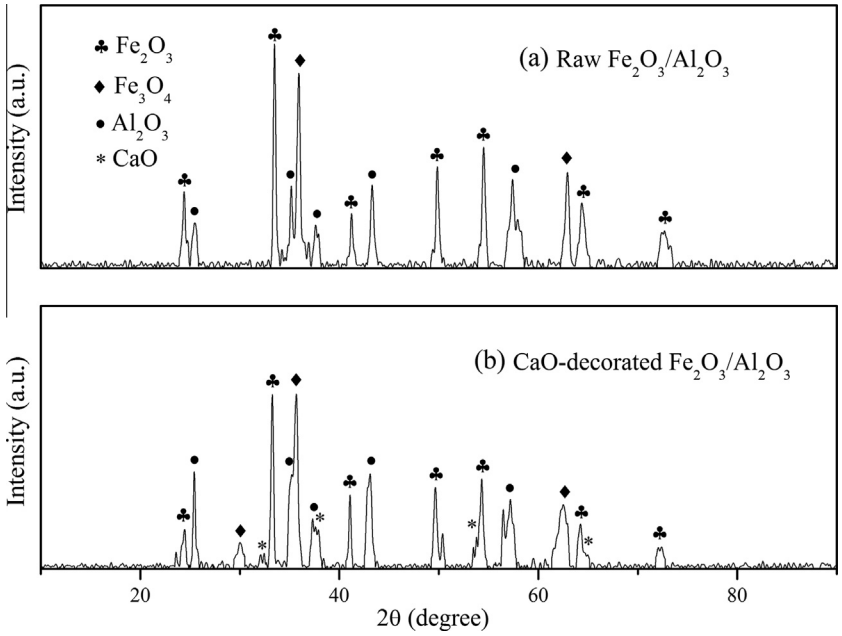

Fig. 7. Phase composition of the reduced status of (a) raw Fe_2O_3/Al_2O_3 and (b) CaO-decorated Fe_2O_3/Al_2O_3.

without CaO decoration. Generally, CaO has a greater BET area [42] and pore volume [43] than Fe_2O_3/Al_2O_3 OCs, which should be responsible for this result. Second, it was found that the BET area (2.61 m^2/g) of used Fe_2O_3/Al_2O_3 OCs is slightly less than that of fresh Fe_2O_3/Al_2O_3 OCs, which should be derived from little ash deposition and slight sintering at successive high-temperature processes. Correspondingly, pore volume (12.35×10^{-3} cm^3/g) of used Fe_2O_3/Al_2O_3 OCs is obviously less than that of fresh Fe_2O_3/Al_2O_3 OCs, which indicated that ash has blocked the pore of OC particles. Note that the BET area and pore volume (BET = 1.86 m^2/g; Pore volume = 10.60×10^{-3} cm^3/g) of 5 wt.% CaO-decorated Fe_2O_3/Al_2O_3 particles after ten successive cycles were distinctly reduced, compared to those fresh 5 wt.% CaO-decorated Fe_2O_3/Al_2O_3 OCs. The reasonable explanation is that ash and part CaO migrated into the pores of Fe_2O_3/Al_2O_3 particles.

3.6.3. SEM–EDX characterization

As shown in Fig. 8(a) and (b), Fe, Al, C, O, Ca and Si were detected in both particles. Among these elements, C was derived from coating the samples with carbon to enhance the sample's electrical conductivity. Integrated with the ash analysis of the medical plastics (Table 2), Ca and Si should be derived from ash deposition for raw Fe_2O_3/Al_2O_3OC particles (shown in Fig. 8(a)). Besides, chlorine was detected on the surface of CaO-decorated OCs after 10 redox cycles (Fig. 8(b)), whereas it was not found on the non-decorated OC surface (Fig. 8(a)). This observation

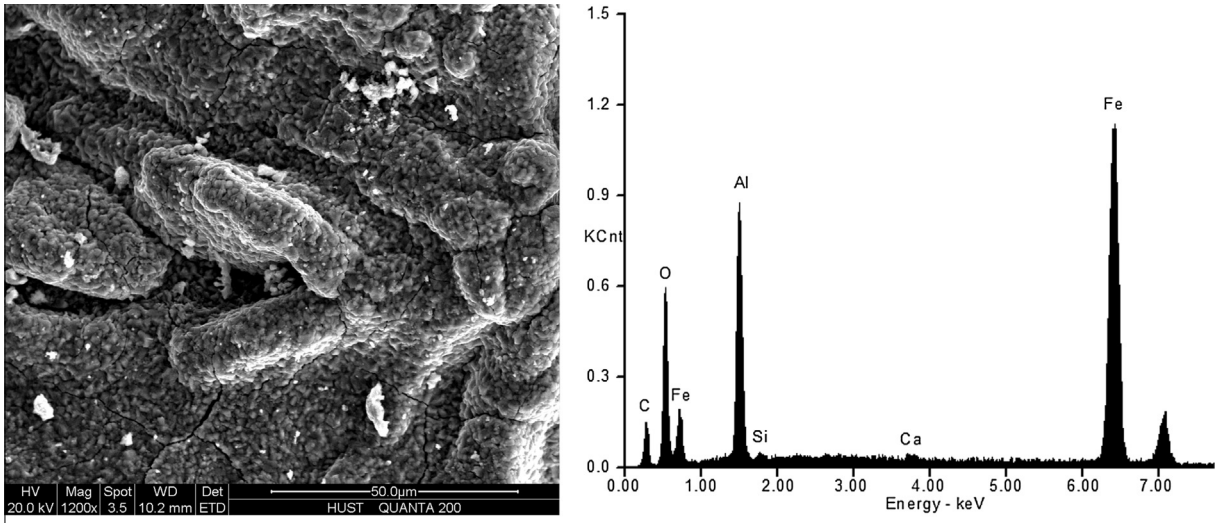

(a) The reduced samples of raw Fe_2O_3/Al_2O_3 particles at the 10th cycle

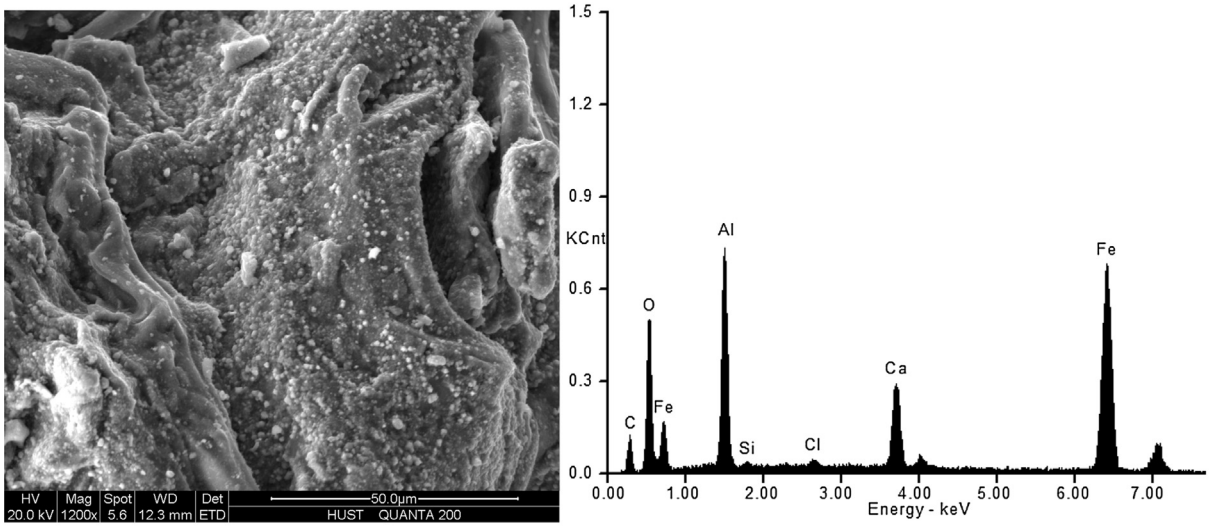

(b) The reduced samples of CaO-decorated Fe_2O_3/Al_2O_3 particles at the 10th cycle

Fig. 8. ESEM images and EDX analysis of different OC particles.

demonstrated that the dechlorination using CaO adsorbent during the iG-CLC process of plastic waste is feasible. Similarly, Si was detected in Fig. 8(b), indicating a little ash deposition on the surface of CaO-decorated OCs. In addition, no obvious sintering/agglomeration has been presented on the surface of these OC particles. Note that these used CaO-decorated OC can be reproduced through being washed by a dilute hydrochloric acid solution and then being decorated again [23].

4. Conclusions

This work first evaluated the reactivity of 5 wt.% CaO-decorated Fe_2O_3/Al_2O_3 as an OC during the iG-CLC process of plastic waste, and the CaO decoration was used for suppressing the Cl-containing components, which possibly help to control the emission of PCDD/Fs. First, the CaO decoration effect was evaluated in a batch fluidized bed reactor through detecting gas compositions in exhaust gas when compared with raw OCs. Following that, operation conditions (including reaction atmosphere, supply oxygen ratio and reactor temperature) were investigated in the same reactor using 5 wt.% CaO-decorated OCs to analyze their effect on carbon conversion, maximum instantaneous rate and CO_2 yield. Results indicate that CaO decoration results in more combustible gases existing from the reactor, and optimizing these operation conditions can obviously improve carbon conversion, maximum instantaneous rate and CO_2 yield. The optimizing operation condition is 900 °C for reaction temperature, 2.5 for supply oxygen ratio, and 40 vol.% steam/60 vol.% N_2 for fluidizing agent. Last, the durability of CaO-decorated OCs reactivity was verified through ten successive redox cycles. No sintering or agglomeration phenomenon occurred and little ash deposited on the surface of OC particles. Notably, the ESEM–EDX result also demonstrated the accumulation of Cl elements on the surface of CaO-decorated Fe_2O_3/Al_2O_3OC particles. In summary, these results demonstrated that in situ dechlorination using CaO-decorated Fe_2O_3/Al_2O_3 OC particles during the utilization of plastic waste as energy is feasible, and iG-CLC process of plastic waste is a promising route for the inhibition of the formation of PCDD/Fs.

In this work, PCDD/Fs cannot be detected in exhaust gas due to a very limited sample used in the batch fluidized-bed reactor experiments. The feasibility of suppressing the formation of

PCDD/Fs would be further examined through detecting the accumulative PCDD/Fs in subsequent continuous iG-CLC experiments of plastic waste.

Acknowledgements

These authors were supported by the "National Natural Science of China (51522603 and 51561125001)". The authors are grateful to the Analytical and Testing Center of HUST for XRD and SEM–EDX measurements.

References

[1] Berguerand N, Lyngfelt A. Design and operation of a 10 kW_{th} chemical-looping combustor for solid fuels – testing with South African coal. Fuel 2008;87:2713–26.
[2] Moldenhauer P, Ryden M, Mattisson T, Lyngfelt A. Chemical-looping combustion and chemical-looping with oxygen uncoupling of kerosene with Mn- and Cu-based oxygen carriers in a circulating fluidized-bed 300 W laboratory reactor. Fuel Process Technol 2012;104:378–89.
[3] Cuadrat A, Cuadrat A, Abad A, Garcia-Labiano F, Gayan P, de Diego LF, et al. Effect of operating conditions in chemical-looping combustion of coal in a 500 Wth unit. Int J Greenhouse Gas Control 2012;6:153–63.
[4] Kim HR, Wang DW, Zeng L, Bayham S, Tong A, Chung E, et al. Coal direct chemical looping combustion process: design and operation of a 25-kW_{th} sub-pilot unit. Fuel 2013;108:370–84.
[5] Leion H, Jerndal E, Steenari BM, Hermansson S, Israelsson M, Jansson E, et al. Solid fuels in chemical-looping combustion using oxide scale and unprocessed iron ore as oxygen carriers. Fuel 2009;88:1945–54.
[6] Cabello A, Abad A, Garcia-Labiano F, Gayan P, de Diego LF, Adanez J. Kinetic determination of a highly reactive impregnated Fe_2O_3/Al_2O_3 oxygen carrier for use in gas-fueled chemical looping combustion. Chem Eng J 2014;258:265–80.
[7] Chiu PC, Ku Y, Wu HC, Kuo YL, Tseng YH. Chemical looping combustion of polyurethane and polypropylene in an annular dual-tube moving bed reactor with iron-based oxygen carrier. Fuel 2014;135:146–52.
[8] Leion H, Mattisson T, Lyngfelt A. The use of petroleum coke as fuel in chemical-looping combustion. Fuel 2007;86:1947–58.
[9] Mattisson T, Leion H, Lyngfelt A. Chemical-looping with oxygen uncoupling using CuO/ZrO_2 with petroleum coke. Fuel 2009;88:683–90.
[10] Gayan P, Adanez-Rubio I, Abad A, de Diego LF, Garcia-Labiano F, Adanez J, et al. Development of Cu-based oxygen carriers for chemical-looping with oxygen uncoupling (CLOU) process. Fuel 2012;96:226–38.
[11] Tian HJ, Siriwardane R, Simonyi T, Poston J. Natural ores as oxygen carriers in chemical looping combustion. Energy Fuels 2013;27:4108–18.
[12] Leion H, Lyngfelt A, Johansson M, Jerndal E, Mattisson T. The use of ilmenite as an oxygen carrier in chemical-looping combustion. Chem Eng Res Des 2008;86:1017–26.
[13] Gayan P, de Diego LF, Garcia-Labiano F, Adanez J, Abad A, Dueso C. Effect of support on reactivity and selectivity of Ni-based oxygen carriers for chemical-looping combustion. Fuel 2008;87:2641–50.
[14] Azimi G, Keller M, Mehdipoor A, Leion H. Experimental evaluation and modeling of steam gasification and hydrogen inhibition in chemical-looping combustion with solid fuel. Int J Greenhouse Gas Control 2012;11:1–10.
[15] Song H, Shah K, Doroodchi E, Wall T, Moghtaderi B. Reactivity of Al_2O_3- or SiO_2-supported Cu-, Mn-, and Co-based oxygen carriers for chemical looping air separation. Energy Fuels 2014;28:1284–94.
[16] Nasr S, Plucknett KP. Kinetics of iron ore reduction by methane for chemical looping combustion. Energy Fuels 2014;28:1387–95.
[17] Shen LH, Wu JH, Gao ZP, Xiao J. Reactivity deterioration of NiO/Al_2O_3 oxygen carrier for chemical looping combustion of coal in a 10 kW_{th} reactor. Combust Flame 2009;156:1377–85.
[18] Mei DF, Abad A, Zhao HB, Adanez J, Zheng CG. On a highly reactive Fe_2O_3/Al_2O_3 oxygen carrier for in situ gasification chemical looping combustion. Energy Fuels 2014;28:7043–52.
[19] Pecho J, Schildhauer TJ, Sturzenegger A, Biollaz S, Wokaun A. Reactive bed materials for improved biomass gasification in a circulating fluidised bed reactor. Chem Eng Sci 2008;63:2465–76.
[20] Zhu HM, Jiang XG, Yan JH, Chi Y, Cen KF. TG-FTIR analysis of PVC thermal degradation and HCl removal. J Anal Appl Pyrol 2008;82:1–9.
[21] Stanmore BR. The formation of dioxins in combustion systems. Combust Flame 2004;136:398–427.
[22] Yan M, Li XD, Yang J, Chen T, Lu SY, Buekens AG, et al. Sludge as dioxins suppressant in hospital waste incineration. Waste Manage 2012;32:1453–8.
[23] Wang J, Zhao H. Chemical looping dechlorination through adsorbent-decorated Fe_2O_3/Al_2O_3 oxygen carriers. Combust Flame 2015;162:3503–15.
[24] Lopez-Urionabarrenechea A, de Marco I, Caballero BM, Laresgoiti MF, Adrados A. Dechlorination of fuels in pyrolysis of PVC containing plastic wastes. Fuel Process Technol 2011;92:253–60.
[25] Wang YF, Wang LC, Hsieh LT, Li HW, Jiang HC, Lin YS, et al. Effect of temperature and CaO addition on the removal of polychlorinated dibenzo-p-dioxins and dibenzofurans in fly ash from a medical waste incinerator. Aerosol Air Qual Res 2012;12:191–9.
[26] Yang WJ, Zhao HB, Ma JC, Mei DF, Zheng CG. Copper-decorated hematite as an oxygen carrier for in situ gasification chemical looping combustion of coal. Energy Fuels 2014;28:3970–81.
[27] Kierzkowska AM, Bohn CD, Scott SA, Cleeton JP, Dennis JS, Miiller CR. Development of iron oxide carriers for chemical looping combustion using sol–gel. Ind Eng Chem Res 2010;49:5383–91.
[28] Abad A, Garcia-Labiano F, de Diego LF, Gayan P, Adanez J. Reduction kinetics of Cu-, Ni-, and Fe-based oxygen carriers using syngas ($CO + H_2$) for chemical-looping combustion. Energy Fuels 2007;21:1843–53.
[29] Zhao HB, Liu LM, Wang BW, Xu D, Jiang LL, Zheng CG. Sol–gel-derived NiO/$NiAl_2O_4$ oxygen carriers for chemical-looping combustion by coal char. Energy Fuels 2008;22:898–905.
[30] Zhao HB, Wang K, Fang YF, Ma JC, Mei DF, Zheng CG. Characterization of natural copper ore as oxygen carrier in chemical-looping with oxygen uncoupling of anthracite. Int J Greenhouse Gas Control 2014;22:154–64.
[31] Zhao HB, Mei DF, Ma JC, Zheng CG. Comparison of preparation methods for iron–alumina oxygen carrier and its reduction kinetics with hydrogen in chemical looping combustion. Asia-Pac J Chem Eng 2014;9:610–22.
[32] Monazam ER, Breault RW, Siriwardane R. Reduction of hematite (Fe_2O_3) to wustite (FeO) by carbon monoxide (CO) for chemical looping combustion. Chem Eng J 2014;242:204–10.
[33] Johansson M, Mattisson T, Lyngfelt A, Abad A. Using continuous and pulse experiments to compare two promising nickel-based oxygen carriers for use in chemical-looping technologies. Fuel 2008;87:988–1001.
[34] Gu HM, Shen LH, Xiao J, Zhang SW, Song T, Chen DQ. Iron ore as oxygen carrier improved with potassium for chemical looping combustion of anthracite coal. Combust Flame 2012;159:2480–90.
[35] Xiao R, Song QL, Song M, Lu ZJ, Zhang SA, Shen LH. Pressurized chemical-looping combustion of coal with an iron ore-based oxygen carrier. Combust Flame 2010;157:1140–53.
[36] Singh S, Wu CF, Williams PT. Pyrolysis of waste materials using TGA-MS and TGA-FTIR as complementary characterisation techniques. J Anal Appl Pyrol 2012;94:99–107.
[37] Cuadrat A, Abad A, de Diego LF, Garcia-Labiano F, Gayan P, Adanez J. Prompt considerations on the design of chemical-looping combustion of coal from experimental tests. Fuel 2012;97:219–32.
[38] Niu X, Shen LH, Gu HM, Song T, Xiao J. Sewage sludge combustion in a CLC process using nickel-based oxygen carrier. Chem Eng J 2015;260:631–41.
[39] Yang WJ, Zhao HB, Wang K, Zheng CG. Synergistic effects of mixtures of iron ores and copper ores as oxygen carriers in chemical-looping combustion. Proc Combust Inst 2015;35:2811–8.
[40] Mendiara T, Garcia-Labiano F, Gayan P, Abad A, de Diego LF, Adanez J. Evaluation of the use of different coals in chemical looping combustion using a bauxite waste as oxygen carrier. Fuel 2013;106:814–26.
[41] Wang CB, Wang JX, Lei M, Gao HN. Investigations on combustion and NO emission characteristics of coal and biomass blends. Energy Fuels 2013;27:6185–90.
[42] Sedghkerdar MH, Mahinpey N, Sun ZK, Kaliaguine S. Novel synthetic sol–gel CaO based pellets using porous mesostructured silica in cyclic CO_2 capture process. Fuel 2014;127:101–8.
[43] Angeli SD, Martavaltzi CS, Lemonidou AA. Development of a novel-synthesized Ca-based CO_2 sorbent for multicycle operation: parametric study of sorption. Fuel 2014;127:62–9.